microorganisms

MDPI

Article

Small-Ruminant Faeces and the Caecal Microbiota of Brandt's Voles: A Field Survey of Winter Food Stores and a Laboratory Feeding Trial

Jieru Feng [1,2,3,4], Shanshan Sun [1,2,3,4], Qiancheng Wang [1,2,3,4], Qiqige Buren [1,2,3,4], Xiaoyu Kang [1,2,3,4], Hongqun Sun [1,2,3,4], Zhipeng Chen [1,2,3,4], Qingxuan Liu [1,2,3,4], Shuai Yuan [1,2,3,4], Guohui Ye [1,2,3,4,*] and Heping Fu [1,2,3,4,*]

[1] College of Grassland Science, Inner Mongolia Agricultural University, Hohhot 010011, China; 15247857547@163.com (J.F.); sunshanshan557@163.com (S.S.); 19997630144@163.com (Q.W.); qiqige19981130@163.com (Q.B.); 15847905995@163.com (X.K.); 17852463271@163.com (H.S.); 15847758395@163.com (Z.C.); liuqingxuan1119@126.com (Q.L.); yuanshuai2020@163.com (S.Y.)
[2] East Ujimqin Banner Typical Grassland Pest Prevention and Control of Inner Mongolia Autonomous Region Field Scientific Observation and Research Station, Xilingol, Xilinhot 026000, China
[3] Alxa Left Banner Desert Ecology and Rodent Monitoring Prevention and Control of Inner Mongolia Autonomous Region Field Scientific Observation and Research Station, Alashan, Bayanhot 750300, China
[4] Key Laboratory of Grassland Resources, Ministry of Education, Hohhot 010011, China
* Correspondence: 18394002004@163.com (G.Y.); fuheping@126.com (H.F.)

Abstract

Brandt's vole (*Lasiopodomys brandtii*) is a dominant rodent species in the temperate typical steppe of northern China, facing dual stresses of low temperature and food scarcity during overwintering. Small-ruminant faeces were found alongside plant material in the winter food stores of Brandt's voles. We combined field surveys, a laboratory feeding trial, and 16S rRNA gene amplicon sequencing to document faecal occurrence in food stores, assess voluntary faeces consumption under laboratory conditions, and compare caecal bacterial communities across feeding treatments. The work was carried out in the typical steppe of Xilingol, Inner Mongolia, covering the periods 2019–2022 and 2024–2025. The results are as follows: (1) A total of 34 overwintering burrow systems were investigated across six years, with an overall detection rate of small-ruminant faeces of 85.29%. No significant linear correlation was observed between the storage mass of small-ruminant faeces and total plant food storage ($R^2 = 0.035$, $F = 1.16$, $p = 0.289$, $n = 34$). Small-ruminant faeces were detected in 29 of 34 burrow systems, and their stored mass showed no statistically detectable association with stored plant-food mass after accounting for survey year. Laboratory feeding experiments showed that daily food intake in the pure small-ruminant faeces group was significantly lower than in both the forage group and the forage+small-ruminant faeces group ($p < 0.001$). Mean body mass in the faeces-only group declined to 18.76 ± 0.83 g (mean ± SE) by day 4, when the group reached the predefined humane endpoint and its trial was terminated. Body mass increased in both forage-fed groups over the 21-day trial. (2) The overall PERMANOVA based on Bray–Curtis dissimilarities was significant ($p = 0.001$), and within-group dispersion was greater in the faeces-only group. This group was sampled at its day-4 humane endpoint following low food intake and rapid body mass loss, while both forage-fed groups were sampled on day 21. Differences in sampling time and physiological status limit the attribution of microbiota differences involving the faeces-only group to diet. Chao1 richness was significantly higher in both forage-fed groups than in the faeces-only group. The overall test for Shannon diversity indicated a difference among the three groups. On day 21, the mean relative abundance of *Akkermansia* was 11.06% in the forage-plus-faeces group and 1.40% in the forage-only group. This pairwise

Check for updates

Academic Editor: Todd Riley Callaway

Received: 30 October 2026
Revised: 21 November 2026
Accepted: 25 November 2026
Published: 27 November 2026

Copyright: © 2026 by the authors. Licensee MDPI, Basel, Switzerland. This article is an open access article distributed under the terms and conditions of the Creative Commons Attribution (CC BY) license.

comparison did not reach statistical significance after BH adjustment (adjusted $p = 0.0568$). These findings document the presence of small-ruminant faeces in winter food stores and voluntary faeces consumption under laboratory conditions. The nutritional consequences of this intake and its relevance to overwintering remain unresolved.

Keywords: Brandt's vole; overwintering food hoarding; heterospecific coprophagy; gut microbiota

1. Introduction

Brandt's vole (*Lasiopodomys brandtii*) is a non-hibernating rodent of the temperate steppe of northern China. It collects and stores plant material in underground chambers in autumn, when food can be gathered for the winter [1,2]. Field and enclosure studies have documented cooperative hoarding and differences among individuals in their contributions to food stores [2,3]. In a laboratory study of lactating Brandt's voles, cold exposure increased food intake and thermogenic capacity [4]. Group huddling, in turn, reduced energy requirements during cold exposure in this species [5]. The composition of winter food stores is therefore relevant to the conditions voles face, while the nutritional value of individual stored items requires separate evaluation.

Reingestion of an animal's own faeces (autocoprophagy) and ingestion of faeces from another species (heterospecific coprophagy) represent different routes of exposure to faecal material. Tracer experiments in Brandt's voles have demonstrated reingestion of material previously passed through their own digestive tract [6]. Heterospecific coprophagy has been observed in the wild, including among ring-tailed lemurs [7]. On the Qinghai–Tibetan Plateau, direct observations and the detection of yak DNA in stomach contents provided evidence of yak faeces consumption by plateau pikas (*Ochotona curzoniae*) [8]. These examples establish that heterospecific coprophagy occurs in particular settings. In Brandt's voles, the presence of livestock faeces in an underground food store documents co-occurrence with stored forage, while consumption of that material in the field remains a separate question.

In vivo studies in Brandt's voles show that the gut microbiota can vary with diet, autocoprophagy and thermal conditions. In the enclosure experiment, Firmicutes were less abundant under light sheep grazing than in the ungrazed control, and Actinobacteria were more abundant under both light and moderate grazing [9]. A complementary feeding experiment found that the voles' gut microbiota differed among three forage diets [9]. Precipitation manipulations also shifted forage use and were accompanied by differences in taxa including *Ruminococcus* and *Prevotella* in the field [10]. Experimentally preventing autocoprophagy altered the gut microbiota and reduced acetate concentrations [11]. Cold acclimation in male Brandt's voles was associated with changes in caecal microbiota, short-chain fatty acid concentrations and thermogenesis, and a pair-feeding experiment showed that cold could alter the caecal microbiota independently of increased intake [12]. Together, these studies identify factors that could affect the caecal microbiota when voles are offered forage and small-ruminant faeces.

The bacterial composition of small-ruminant faeces also depends on their source. In an age-matched comparison of sheep and goats, faecal bacterial profiles were broadly similar at the phylum level, and bacterial diversity was higher at 12 months than at 6 months [13]. In goats, pasture grazing and barn feeding were associated with different faecal bacterial communities [14]. Multi-year field sampling also documented variation among sampling years in sheep faecal microbiota and differences before and after grazing in goat faecal microbiota [15]. Thus, the livestock species, source herd, feeding conditions and collection

period are relevant when characterising faeces used in a feeding trial. Any dietary or microbial interpretation should refer to the material sampled or offered in the experiment.

We surveyed Brandt's vole burrow systems to determine how often small-ruminant faeces occurred in winter food stores and whether the stored masses of faeces and plant material were associated after accounting for survey year. In a laboratory feeding trial, we asked whether voles consumed faeces when offered forage and faeces separately, and hypothesised that access to faeces would be associated with differences in caecal bacterial composition relative to the forage-only treatment. We also recorded food intake and body mass and characterised predicted microbial functional profiles.

2. Materials and Methods

2.1. Study Area

The study was carried out at the Inner Mongolia Autonomous Region Field Scientific Observation and Research Station for Typical Steppe Pest Prevention and Control, situated in East Ujimqin Banner, Xilingol League, Inner Mongolia Autonomous Region, China, with a geographic range of 115°30′–116°30′ E and 44°42′–45°15′ N. The grassland in the study area is classified as temperate typical steppe, dominated by high-plain terrain, and has a north temperate continental climate. The mean annual temperature is 1.6 °C, with an extreme maximum temperature of 39.7 °C and an extreme minimum temperature of −40.7 °C [16]. The mean annual precipitation is approximately 300 mm, 70% of which is concentrated between June and August; annual evaporation exceeds 3000 mm. The annual growing period (defined as days with daily mean temperature > 5 °C) lasts 95 days, with a frost-free period of 120 days [16]. Chestnut soil was reported as the predominant soil type at a typical-steppe research site in East Ujimqin Banner [17]. At the study site, vegetation was 10–20 cm tall, and the dominant plant species included *Allium polyrhizum*, *Stipa grandis*, and *Neopallasia pectinata* [2]. A field survey of the grasslands of eastern Inner Mongolia that included East Ujimqin Banner recorded Brandt's voles (*Lasiopodomys brandtii*), striped dwarf hamsters (*Cricetulus barabensis*), Daurian ground squirrels (*Spermophilus dauricus*), and Mongolian gerbils (*Meriones unguiculatus*). Brandt's voles were the most frequently captured species, accounting for 44.64% of all rodents captured across the eight survey sites [18].

2.2. Experimental Design

To conduct long-term dynamic analysis, we integrated systematic monitoring data collected from 2019 to 2022. This study was carried out in October 2024 at the Inner Mongolia Autonomous Region Field Scientific Observation and Research Station for Typical Steppe Pest Prevention and Control in East Ujimqin Banner. Over two consecutive overwintering periods, we excavated Brandt's vole burrow systems and classified and recorded the composition of food stores in their storage chambers. Subsequently, a laboratory feeding trial was conducted to assess voluntary consumption of small-ruminant faeces and to compare caecal bacterial profiles among feeding treatments. The experimental Brandt's voles (*Lasiopodomys brandtii*) were healthy subadults weighing 21–30 g, captured from the typical steppe region. Each Brandt's vole was housed singly in an individually ventilated cage under controlled environmental conditions: a temperature of 20 ± 1 °C, a relative humidity of 40–60%. The voles underwent a 7-day acclimation period with ad libitum access to basal forage and drinking water, and entered the formal experiment after their stable health status was confirmed (free of ectoparasites and abnormal clinical signs). A one-week acclimation period under a 14 h light and 10 h dark cycle has also been used in a previous study of the gut microbiota of Brandt's voles [19].

Before the formal feeding trial, we conducted a feasibility pilot to observe food intake and changes in body mass in Brandt's voles offered the experimental diets. The pilot did not include 16S rRNA gene sequencing and therefore did not provide an effect-size estimate for the relative abundance of *Akkermansia*. A controlled feeding study in postweaning Brandt's voles compared gut microbial composition across diets differing in plant species richness and composition [20]. Food intake and body mass have also been monitored in this species in experiments that prevented autocoprophagy [11] or manipulated ambient temperature and food intake through pair-feeding [12]. These studies provide methodological precedents for monitoring feeding responses alongside gut microbiota profiling.

A total of 21 Brandt's voles were stratified by body weight and randomly assigned to three dietary groups ($n = 7$ per group). The groups were forage only (XC), forage plus small-ruminant faeces (XC_F), and small-ruminant faeces only (YF). The YF group was included to document food intake and changes in body mass when small-ruminant faeces were the sole feed available. The sex composition of each group was as follows: 2 females and 5 males in the XC group, 4 females and 3 males in the XC_F group, and 2 females and 5 males in the YF group. Because sex composition differed among groups, sex was included in selected statistical models as described in Section 2.4.2. Group assignment was performed by personnel not involved in subsequent indicator measurements to ensure randomization and allocation concealment.

Voles in the forage-only group (XC) were offered a mixture of six plant species: *Neopallasia pectinata*, *Leymus chinensis*, *Allium polyrhizum*, *Potentilla bifurca*, *Stipa grandis*, and *Carex tristachya*. Voles in XC_F had ad libitum access to the same forage mixture provided to XC and to small-ruminant faeces offered in a separate feeder. The two feeds were offered on a free-choice basis, with no predetermined mixing ratio. Leftover forage and faeces were collected daily, and intake of each was calculated separately using the moisture correction described in Section 2.3. Voles in the faeces-only group (YF) were fed exclusively on small-ruminant faeces. Fresh small-ruminant faeces used in the experiment were collected from free-grazing sheep and goats within the study area. After removing plant debris and impurities, the faecal samples were stored at 4 °C under refrigeration. Moisture content was calibrated prior to feeding, and no sterilization treatment was applied to preserve the indigenous microbiota in the faeces. Before the start of the formal experiment, the moisture content of the experimental forage plants and small-ruminant faeces was calibrated, and daily food intake of each vole was recorded throughout the experiment. The designed experimental duration was 21 days. The pure small-ruminant faeces group was terminated early when the animals reached the predefined humane endpoint, while the other two groups completed the full experimental period. Caecal content samples were collected from all experimental voles at the end of the experiment.

2.3. Determination Indicators and Methods

Food storage composition analysis: Food hoards in field burrow systems were classified by plant species and small-ruminant faeces, and weighed after drying to constant weight.

Daily food intake and body weight monitoring: Daily food intake was measured on a fresh weight basis, with simultaneous moisture correction to eliminate bias caused by natural water loss of forage. Before feeding, the fresh weight of forage supplied on the day was weighed and recorded as the provided amount A; after the 24 h feeding cycle, the remaining forage in the cage was collected and weighed for fresh weight, recorded as the residual amount B. Moisture calibration parallel samples were prepared daily: three biological replicates were set up using the same batch of forage. The initial fresh weight of each calibration sample was recorded as X; after 24 h of static placement under conditions identical to the housing environment, the final fresh weight was recorded as Y. The moisture

correction factor was calculated as the mean of the three replicates: correction factor = Y/X, representing the weight retention ratio of forage after 24 h of environmental exposure.

The actual daily food intake (N) per individual was calculated as follows:

$$N = A \times \frac{Y}{X} - B$$

Note: In the forage-plus-faeces group (XC_F) and the faeces-only group (YF), small-ruminant faeces intake was estimated for each vole. The fresh mass of the faeces offered was measured before each 24 h feeding period. Uneaten faeces were collected and weighed at the end of the period. In XC_F, forage and faeces were offered separately, and the leftovers of each feed type were weighed separately. Daily faeces intake (g per vole per day) was estimated by multiplying the initial fresh mass of faeces offered by the 24 h mass retention fraction for faeces and subtracting the fresh mass of the leftovers. The mass retention fraction was calculated as the ratio of final to initial mass in control samples from the same faecal batch, held under the same conditions for 24 h without access by the voles.

Gut microbiota sequencing: Caecal contents were collected after euthanasia at the respective endpoints described in Section 2.5. Dissection tools were placed in sterilized trays, and both the trays and tools were sprayed with anhydrous ethanol and immediately ignited for dry-heat sterilization. Caecal contents of the voles were transferred into 2 mL sterile cryopreservation tubes, labelled, and stored at −80 °C. Masks and sterile gloves were worn throughout the sampling process. It was ensured that dissection tools were re-sterilized and sterile gloves were replaced before sampling each individual animal, with the sterilization procedure repeated for each sample. Three replicate subsamples from the same batch of sheep faeces used in the feeding trial (F1) were profiled by 16S rRNA gene amplicon sequencing for descriptive comparison with the vole caecal samples.

(1) Total Microbial Genomic DNA Extraction

Total microbial genomic DNA was extracted from caecal content samples using a magnetic bead-based faecal genomic DNA extraction kit (AU46111-96, BioTeke, Beijing, China), with operations performed strictly in accordance with the kit instructions. DNA concentration was determined using a Qubit fluorometer (Invitrogen, Carlsbad, CA, USA), and DNA integrity was verified by agarose gel electrophoresis. Qualified samples were used for subsequent PCR amplification. Full-process negative controls covering DNA extraction and PCR amplification were not included in this study. No verifiable negative-control results were available for reporting.

(2) PCR Amplification and Product Purification

The V3–V4 variable region of the bacterial 16S rRNA gene was selected as the amplification target, and amplification was carried out using the universal primers 341F (5′-CCTACGGGNGGCWGCAG-3′) and 805R (5′-GACTACHVGGGTATCTAATCC-3′). The PCR reaction system (total volume 25 μL) contained 12.5 μL of Phusion Hot Start Flex 2× Master Mix (New England Biolabs, Ipswich, MA, USA), 2.5 μL each of forward and reverse primers (5 μmol/L), 50 ng of template DNA, and sterile ultrapure water to bring the final volume to 25 μL.

The amplification procedure was as follows: initial denaturation at 98 °C for 30 s; 32 cycles of denaturation at 98 °C for 10 s, annealing at 54 °C for 30 s, and extension at 72 °C for 45 s; and a final extension at 72 °C for 10 min, followed by storage at 4 °C. The amplified products were purified using AMPure XT magnetic beads (Beckman Coulter Genomics, Danvers, MA, USA) and accurately quantified with a Qubit fluorometer.

(3) Library Construction and High-Throughput Sequencing

The quality of purified products was evaluated using an Agilent 2100 Bioanalyzer (Agilent Technologies, Santa Clara, CA, USA) and an Illumina Library Quantification Kit (KAPA Biosystems, Woburn, MA, USA). Qualified libraries were required to reach a concentration of 2 nmol/L or above. Qualified libraries were serially diluted according to sequencing requirements, pooled in equal volumes, denatured into single strands with NaOH, and subjected to paired-end 250 bp (PE250) high-throughput sequencing on the Illumina NovaSeq 6000 platform (Illumina, San Diego, CA, USA) by LC Bio Technology Co., Ltd. (Hangzhou, China).

2.4. Data Processing

2.4.1. Bioinformatic Analysis

A total of 21 caecal content samples were included in this study for 16S rRNA high-throughput sequencing. All samples passed quality control filtering and were retained for subsequent bioinformatic analysis. The raw sequencing reads from these 21 caecal samples were deposited in the NCBI Sequence Read Archive (BioProject: PRJNA1565328; SRA Study: SRP758050). Bioinformatic analysis of raw sequencing data was performed using the standard 16S rRNA analysis pipeline of LC Bio Technology Co., Ltd. (Hangzhou, China), with the core analytical framework built on the QIIME 2 platform. First, quality control was conducted on paired-end raw reads: low-quality sequences with an average quality score below 20 and a length shorter than 200 bp were discarded, and primer sequences were trimmed using Cutadapt (v1.9). Subsequently, the DADA2 algorithm was applied for sequence denoising, base error correction, and chimera removal to generate Amplicon Sequence Variants (ASVs). A Venn diagram was constructed based on the ASV table to display shared and unique sequences among groups. Taxonomic classification was performed against the SILVA database (Release 138) with a confidence threshold of 0.7, covering five taxonomic ranks: phylum, class, order, family, and genus. The top 20 taxa in terms of relative abundance at each taxonomic level were selected to generate stacked bar plots of species composition and z-score-normalized abundance heatmaps. For alpha diversity comparisons, all samples were rarefied to 49,679 sequences per sample. Chao1 richness and Shannon diversity were calculated from the rarefied ASV table. Shannon rarefaction curves were used to assess whether diversity estimates stabilised as sequencing depth increased. Beta diversity analysis was performed based on Bray–Curtis distance, including Principal Coordinates Analysis (PCoA) and Analysis of Similarities (ANOSIM). Microbial functional profiles were predicted from 16S rRNA gene amplicon data using PICRUSt2 (v2.6.2). Based on the KEGG database, abundance tables of KEGG Orthology (KO), as well as level 1, level 2 and level 3 KEGG metabolic pathways were generated. Predicted MetaCyc pathway abundances were obtained from the PICRUSt2 output. For carbohydrate-active enzyme (CAZyme) families, ASV representative sequences were placed in the reference phylogenies of the bundled PICRUSt2-SC database. Hidden-state prediction was used to estimate 16S rRNA gene copy numbers and CAZyme family gene copy numbers for each ASV. Within each sample, the predicted abundance of each CAZyme family was calculated by multiplying the 16S rRNA gene copy number-corrected abundance of each ASV by its predicted copy number for that family and summing across ASVs. The resulting family abundances were converted to within-sample relative abundances by total-sum scaling (TSS) before downstream analysis. Differential analysis of functional profiles among the three groups (XC: forage group; XC_F: forage + small-ruminant faeces group; YF: faeces-only group) was performed as follows: overall differences across multiple groups were tested using the Kruskal–Wallis rank-sum test, and pairwise comparisons between groups were conducted using the Wilcoxon rank-sum test. The Benjamini–Hochberg (BH) method

was applied for multiple testing correction, with a significance threshold set at $p < 0.05$. LEfSe analysis was performed to identify group-associated functional biomarkers, using the one-against-all multi-class comparison strategy. Briefly, differential features were first screened by the Kruskal–Wallis test, then validated by pairwise Wilcoxon rank-sum tests, and finally the effect size was estimated by linear discriminant analysis (LDA). An LDA score threshold of 2.0 and a significance threshold of $p < 0.05$ were applied. BH-adjusted q-values were calculated for all differential pathways in the output table.

2.4.2. Statistical Analysis

Statistical analyses were performed in R (version 4.4.1, R Foundation for Statistical Computing, Vienna, Austria). Pairwise comparisons of taxon and predicted functional pathway relative abundances were performed using two-sided Wilcoxon rank-sum tests with Benjamini–Hochberg (BH) adjustment. For *Akkermansia*, BH adjustment was applied across the three pairwise comparisons with sexes pooled. A Scheirer–Ray–Hare test was used to assess the associations of dietary group, sex, and their interaction with *Akkermansia* relative abundance. In exploratory analyses, pairwise Wilcoxon rank-sum tests were repeated separately for females and males, with BH adjustment across the three comparisons within each sex. The significance threshold was 0.05. For inter-group comparisons of phenotypic indicators such as daily food intake and body weight, as well as gut microbiota alpha diversity indices, one-way analysis of variance (one-way ANOVA) combined with Tukey's HSD post hoc test was used. To exclude the confounding effect of unbalanced sex distribution among the three groups, sex was further included as a covariate in analysis of covariance (ANCOVA), and Type III sum of squares main effects were calculated via the 'car' package. For repeated-measurement phenotypic data (daily body weight and daily food intake), linear mixed-effects models (LMMs) were constructed using the 'lme4' and 'lmerTest' packages in R to explicitly account for within-individual correlation across sequential observations. Dietary group, experimental day, and their two-way interaction were set as fixed effects, with sex included as a covariate to control for confounding from unbalanced sex distribution. Individual animal identity was specified as a random intercept to model non-independence of repeated measurements from the same subject. Type III Wald chi-square tests were used to evaluate the statistical significance of all fixed effects. The first four days provided a common observation window for comparing daily food intake and body mass across the three groups. Daily food intake was also analysed over the full 21-day trial in XC and XC_F, the two groups that completed the trial. Final body mass on day 21 was compared separately between XC and XC_F, with sex included as a covariate. Unless otherwise specified, all phenotypic values in the text and figures are presented as mean ± standard error (SE), and the significance threshold was uniformly set at $p < 0.05$. Differences in caecal microbial community composition among dietary groups were assessed by PERMANOVA and ANOSIM using Bray–Curtis dissimilarities in the R package vegan, with 999 permutations for each test. We also fitted a marginal PERMANOVA including dietary group and sex as predictors. Homogeneity of multivariate dispersion among groups was assessed by PERMDISP using Bray–Curtis dissimilarities. Pairwise differences in dispersion were evaluated using Tukey's HSD procedure. Figures were generated and refined using the ggplot2 package in R and OriginPro (version 2026b SR2, OriginLab Corporation, Northampton, MA, USA).

2.5. Animal Ethics

The animal experimental protocol of this study was reviewed and approved by the Laboratory Animal Ethics Committee of Inner Mongolia Agricultural University. All procedures were performed in strict compliance with animal ethics guidelines (see the Ethics

Approval Statement for details). During the experiment, the general state and feeding behavior of the animals were monitored daily. A body weight loss exceeding 20% of the baseline body weight was predefined as the humane endpoint criterion. The YF trial was terminated on day 4 when the predefined humane endpoint was reached, and the animals in that group were euthanised on that day. Voles in XC and XC_F were euthanised at the scheduled end of the trial on day 21. In all groups, euthanasia was performed by trained personnel using cervical dislocation. All operations strictly followed the 3Rs principles of Replacement, Reduction and Refinement. The completed ARRIVE 2.0 Checklist [21] is provided in the Supplementary Materials.

3. Results

3.1. Field and Laboratory Verification of Overwintering Small-Ruminant Faeces Hoarding in Brandt's Voles

3.1.1. Small-Ruminant Faeces Hoarding Phenomenon Revealed by Historical Data

A total of 22 burrow systems were surveyed during the investigation period from 2019 to 2022, among which small-ruminant faeces were detected in 18 burrow systems, with an overall detection rate of 81.8%. The detection rate of small-ruminant faeces was 100.00% in 2019, decreased to 50.00% in 2020, rebounded to 100.00% in 2021, and slightly declined to 80.00% in 2022 (Figure 1). Overall, with the exception of the relatively low detection rate in 2020, the detection rates remained at 80% or above in other years, with full detection achieved in 2019 and 2021. Additional field surveys were conducted in 2024 and 2025 to quantify the detection of small-ruminant faeces in surveyed burrow systems in each year. In 2024, 6 burrow systems were investigated, among which 5 contained stored small-ruminant faeces, corresponding to a storage rate of 83.33%. In 2025, 6 burrow systems were also surveyed, and small-ruminant faeces storage was identified in all burrow systems, with a storage rate of 100.00%. A total of 12 burrow systems were investigated across the two years, with an overall storage rate of 91.67%.

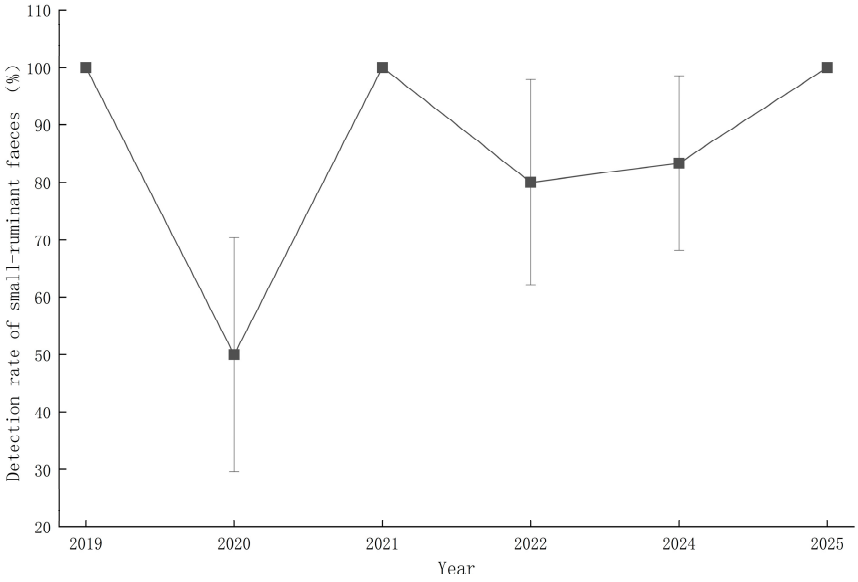


Figure 1. Detection rate of small-ruminant faeces in burrow systems.

3.1.2. Relationship Between Small-Ruminant Faeces Storage Mass and Plant Food Storage Mass

Across the 34 burrow systems, the relationship between plant-food storage mass and small-ruminant-faeces storage mass was first examined using an unadjusted ordinary least-

squares regression. The raw-scale model was not statistically significant ($R^2 = 0.0351$, $F_{(1,32)} = 1.163$, $p = 0.289$). For the raw-scale OLS model, the Shapiro–Wilk test indicated a departure from residual normality ($W = 0.607$, $p < 0.001$), and the studentized Breusch–Pagan test yielded $p = 0.184$. Two observations from 2019 exceeded the $4/n$ reference threshold for Cook's distance (Figure S1C). Because faeces-storage mass was right-skewed, included zero values, and showed marked interannual heterogeneity, the primary analysis used a log1p-transformed linear mixed-effects model with year included as a random intercept. Plant-food storage mass was not significantly associated with faeces-storage mass in the year-aware model ($\beta = -0.043$, 95% CI: −0.493 to 0.407, $p = 0.847$; Figure 2A). Year-stratified ordinary least-squares regressions are presented in Figure 2B. Marginal residual diagnostics for the mixed-effects model are shown in Figure S1A,B. This conclusion remained unchanged after excluding all six observations from 2019, using a year-fixed-effects model ($\beta = -0.028$, 95% CI: −0.466 to 0.410, $p = 0.897$). A two-part analysis also showed no significant association between plant-food storage mass and faeces presence or absence ($p = 0.686$) or positive faeces-storage mass among burrow systems containing faeces ($\beta = -0.121$, $p = 0.673$).

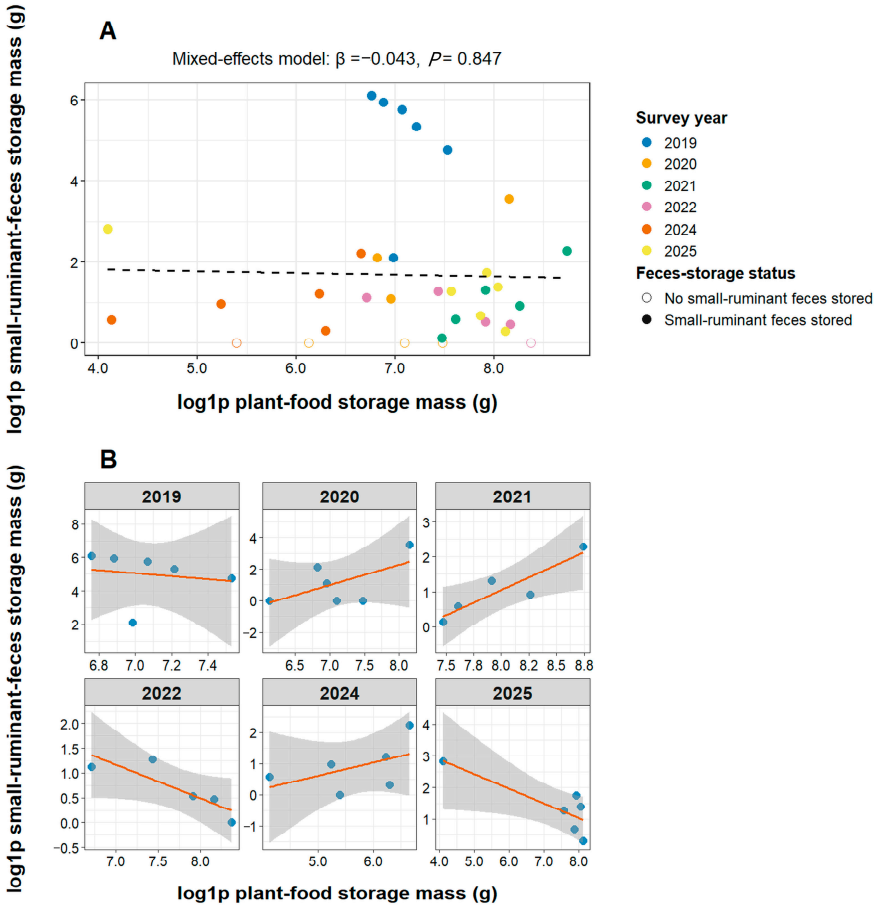


Figure 2. Association between plant food storage mass and small-ruminant faeces storage mass in Brandt's vole burrow systems. (**A**) Overall relationship fitted by a linear mixed-effects model with survey year as a random intercept, based on log1p-transformed data. Open circles indicate burrow systems with no stored small-ruminant faeces, and filled circles indicate burrow systems with positive faeces storage. The dashed line represents the marginal fitted line of the fixed effect of plant storage mass. (**B**) Year-stratified ordinary least squares (OLS) regressions for each survey year. Orange lines and grey shaded areas represent fitted regression lines and 95% confidence intervals, respectively.

Statistical analysis of the proportion of small-ruminant faeces in the food stores of Brandt's vole burrow systems across 2019–2022 and 2024–2025 demonstrated prominent interannual variation in this metric (Table 1). Overall, the proportion of small-ruminant faeces was relatively high in 2019, with a mean value of 17.13%, which was significantly higher than that in all other years. A high degree of dispersion was observed in 2019, with the proportion ranging from 0.67% to 34.19% among individual burrow systems. The annual mean proportion of small-ruminant faeces was below 1% in 2020, 2021, 2022, and 2024, with the lowest mean recorded in 2021 (0.07%). In 2025, the mean proportion was 3.61%, and the maximum recorded in an individual burrow system was 21.23%.

Table 1. Mean proportion of small-ruminant faeces in food stores of Brandt's vole burrow systems, 2019–2022 and 2024–2025.

Year	Burrow Systems (*n*)	Mean Proportion of Small-Ruminant Faeces (%, Mean ± SE)	Range (%)
2019	6	17.13 ± 5.28 a	0.67~34.19
2020	6	0.32 ± 0.18 b	0~0.96
2021	5	0.07 ± 0.02 b	0.01~0.14
2022	5	0.09 ± 0.05 b	0~0.26
2024	6	0.62 ± 0.21 b	0~1.26
2025	6	3.61 ± 3.52 b	0.01~21.23

Note: Data are expressed as mean ± standard error (SE). A total of 34 burrow systems were surveyed across 2019–2022 and 2024–2025, and the number of burrow systems investigated each year is presented in the table. Different lowercase letters in the same column indicate significant differences among groups ($p < 0.05$, one-way ANOVA followed by Tukey's post hoc test).

3.1.3. Differences in Total Daily Food Intake and Average Consumption of Different Food Combinations

Daily food intake trajectories across the three dietary treatments are shown in Figure 3. Voles in the XC and XC_F groups maintained relatively stable but fluctuating food intake throughout the 21-day experimental period, with an overall upward trend as body weight increased. In contrast, the YF group exhibited a continuous decline in daily food intake and was terminated on day 4 when animals reached the predefined humane endpoint. Linear mixed-effects model analysis of the first 4 days (the common observation window for all groups) showed a highly significant main effect of dietary treatment on daily food intake ($\chi^2 = 45.48$, df = 2, $p < 0.001$) and a significant Group × Day interaction effect ($\chi^2 = 7.37$, df = 2, $p = 0.025$). No significant main effect of day ($p = 0.144$) or sex ($p = 0.724$) was detected over this period. For the two groups completing the full 21-day experiment, the main effect of dietary treatment remained highly significant across the entire period ($\chi^2 = 15.98$, df = 1, $p < 0.001$). Food intake increased significantly over time in both groups ($\chi^2 = 20.93$, df = 1, $p < 0.001$), and the significant Group × Day interaction indicated different rates of intake increase between the two treatments ($\chi^2 = 11.75$, df = 1, $p < 0.001$). Over the 21-day trial, mean daily food intake was 12.10 ± 0.39 g in the forage-only group (XC) and 10.92 ± 0.23 g in the forage-plus-faeces group (XC_F) (mean ± SE). The post hoc comparison showed higher intake in XC than in XC_F ($p < 0.05$). Mean daily food intake in the faeces-only group (YF) was 2.35 ± 0.12 g over its four-day observation period (Figure 3).

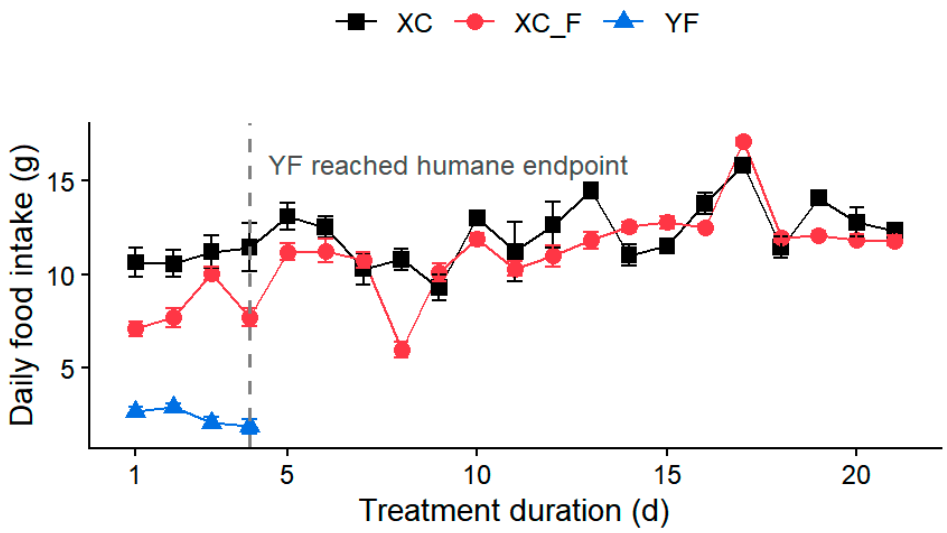


Figure 3. Daily food intake trajectories of Brandt's voles across the three dietary treatments. Note: Values are presented as mean ± standard error (SE). The YF group was terminated early on day 4 when animals reached the predefined humane endpoint; thus, only data from days 1 to 4 are available for this group. The grey dashed line indicates the termination time point of the YF group. XC: forage group; XC_F: forage + small-ruminant faeces group; YF: small-ruminant faeces-only group.

Consumption was quantified separately for each of the six forage species listed in Section 2.2 and for small-ruminant faeces. The average daily consumption (g/day) of each food type was quantified across the three treatment groups (XC, XC_F, YF). Among all plant items, *N. pectinata* had the highest daily consumption in both the XC and XC_F groups, at 8.341 g/day and 6.897 g/day, respectively, which was markedly higher than that of all other plant species. *A. polyrhizum* and *L. chinensis* ranked second in consumption: daily intake of *A. polyrhizum* was 1.373 g in the XC group and 1.195 g in the XC_F group, while that of *L. chinensis* was 1.294 g and 1.262 g, respectively, with only minor differences between the two groups. Consumption of *P. bifurca* remained at similar levels between treatments, at 0.650 g/day in the XC group and 0.622 g/day in the XC_F group. Consumption of *S. grandis* and *C. tristachya* was relatively low overall, but both were slightly higher under the XC_F treatment than under the XC treatment: *S. grandis* intake increased from 0.304 g/day to 0.343 g/day, and *C. tristachya* intake rose from 0.137 g/day to 0.242 g/day. Voles in XC_F consumed a mean of 0.362 g of small-ruminant faeces per day, corresponding to approximately 3.3% of the group's mean total daily food intake by mass. Mean daily faeces intake in YF was 2.351 g over its four-day observation period (Figure 4). The YF group reached the predefined humane endpoint on day 4. Daily food intake was lower in XC_F than in XC, and body mass increased in both forage-fed groups over the 21-day trial.

3.1.4. Body Weight Changes of Brandt's Voles with Small-Ruminant Faeces Intake

The body weight trends of Brandt's voles in the three groups during the feeding period are shown in Figure 5. Body weight in the control group (XC) and the small-ruminant faeces-supplemented group (XC_F) exhibited a continuous increasing trend over the 21-day feeding cycle. In contrast, body weight in the pure small-ruminant faeces group (YF) showed progressive decline, and the experiment was terminated on day 4 of feeding when the animals reached the predefined humane endpoint. Two-way analysis of covariance (ANCOVA) was applied to verify the baseline balance of initial body weight on day 1. The results showed no significant difference in initial body weight among the three groups ($F_{(2,15)} = 0.40$, $p > 0.05$), and sex exerted no significant main effect on initial body weight ($F_{(1,15)} = 1.76$, $p > 0.05$), indicating consistent body weight baselines across all groups. Only

data from the first 4 days were adopted to compare the rate of body weight change across the three groups over the same period, with initial body weight and sex included in the model as covariates for adjustment. After correction for the two covariates, the rate of body weight change over the first 4 days remained highly significantly different among the three groups ($F_{(2,14)} = 37.28$, $p < 0.001$). Neither initial body weight ($p > 0.05$) nor sex ($p > 0.05$) exhibited a significant main effect. The linear mixed-effects model for daily body mass showed a dietary group × day interaction ($\chi^2 = 117.51$, $df = 2$, $p < 0.001$). In a separate comparison on day 21, final body mass did not differ significantly between XC and XC_F after adjustment for sex ($F_{(1,11)} = 4.19$, $p = 0.065$). Sex was not significantly associated with final body mass ($p = 0.172$).

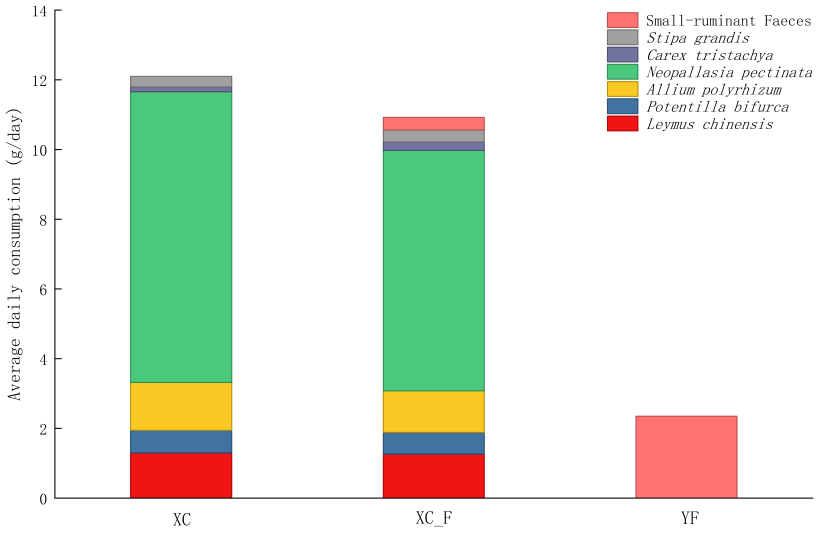


Figure 4. Daily consumption of small-ruminant faeces and six plant species in the three groups.

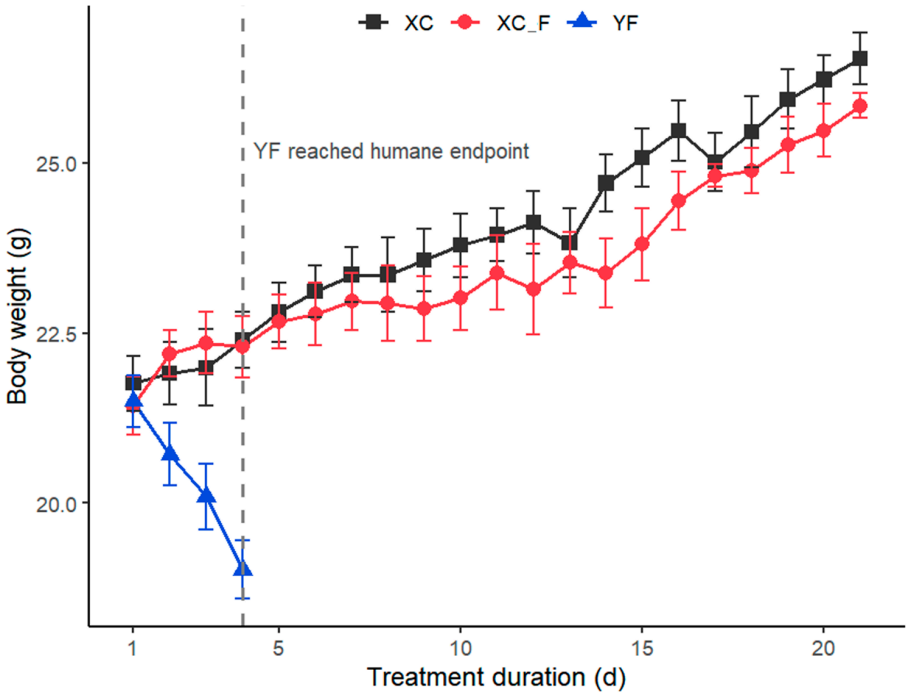


Figure 5. The changes in weight of the three groups during the experiment. Note: Points show group means, and error bars indicate standard errors (SE). The faeces-only group (YF) was followed through day 4.

3.2. Effects of Different Food Combinations on Gut Microbiota of Brandt's Voles

3.2.1. Sequencing Results of Gut Microbiota in Brandt's Voles Across Different Groups

The sequencing data of the 21 caecal content samples in this study met the quality requirements, and all were subjected to downstream diversity and taxonomic composition analysis. The ASV composition of each sample group was analyzed via a Venn diagram (Figure 6A). The results showed that there were 2479 unique ASVs in the XC group, 2286 unique ASVs in the XC_F group, and 1524 unique ASVs in the YF group. The proportions of shared ASVs between the YF group and the XC group, and between the YF group and the XC_F group were 3.16% and 2.74%, respectively, both at relatively low levels. The proportion of shared microbial taxa between the XC group and the XC_F group reached 13.49%, indicating higher similarity in community composition between the two groups. The Shannon rarefaction curves approached a plateau as sequencing depth increased (Figure 6B).

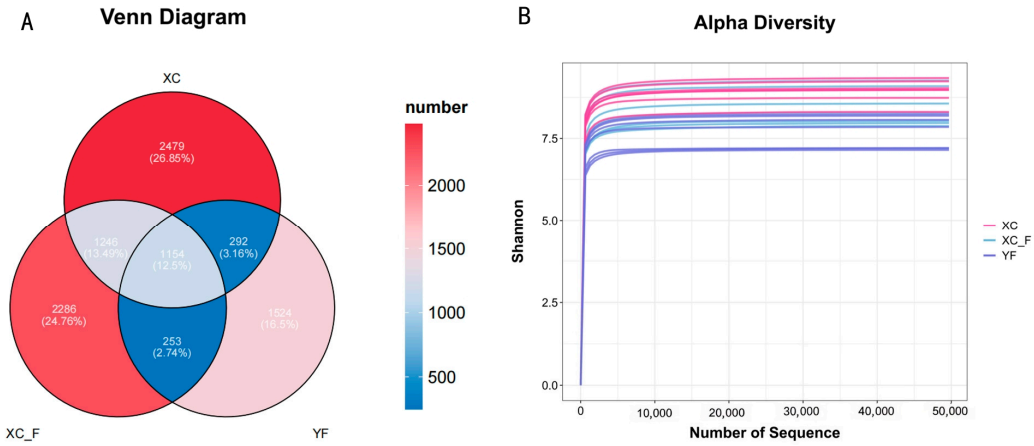


Figure 6. (**A**) Venn diagram of the number of intestinal ASVs in different groups. (**B**) Rarefaction curves of intestinal microbiota.

3.2.2. Gut Microbiota Species Composition of Brandt's Voles Across Different Groups

Inter-group differences in taxon abundance were tested using the Wilcoxon rank-sum test, with multiple comparisons corrected via the Benjamini–Hochberg (BH) method. The stacked bar plot of gut microbiota relative abundance at the phylum level (Figure 7) showed that all detected bacterial phyla across the XC, XC_F, and YF groups belonged to the domain Bacteria. Distinct inter-group differences were observed in the phylum-level structural composition of the microbiota and in the relative abundance of core dominant phyla. Firmicutes was the absolute dominant phylum in all three groups, with relative abundances of 68.13% in the XC group, 65.90% in the XC_F group, and 54.39% in the YF group, presenting a decreasing trend of XC > XC_F > YF. Bacteroidota was the second most dominant phylum across all groups; its relative abundance rose significantly to 29.91% in the YF group, far exceeding the levels in the XC group (16.35%) and the XC_F group (12.20%). Desulfobacterota maintained a relatively high abundance in all three groups, with relative abundances of 9.02% (XC group), 6.53% (XC_F group), and 10.79% (YF group), respectively. The abundance of Verrucomicrobiota was specifically elevated in the XC_F group, reaching 11.07%, which was significantly higher than that in the XC group (1.40%) and the YF group (0.64%). In addition, the relative abundances of Actinobacteriota and Proteobacteria were all below 2.5% in each group. Except for the aforementioned phyla, the relative abundances of other detected phyla were less than 1% in all groups. These were classified as low-abundance rare phyla and accounted for an extremely small proportion of the overall microbiota composition of each group.

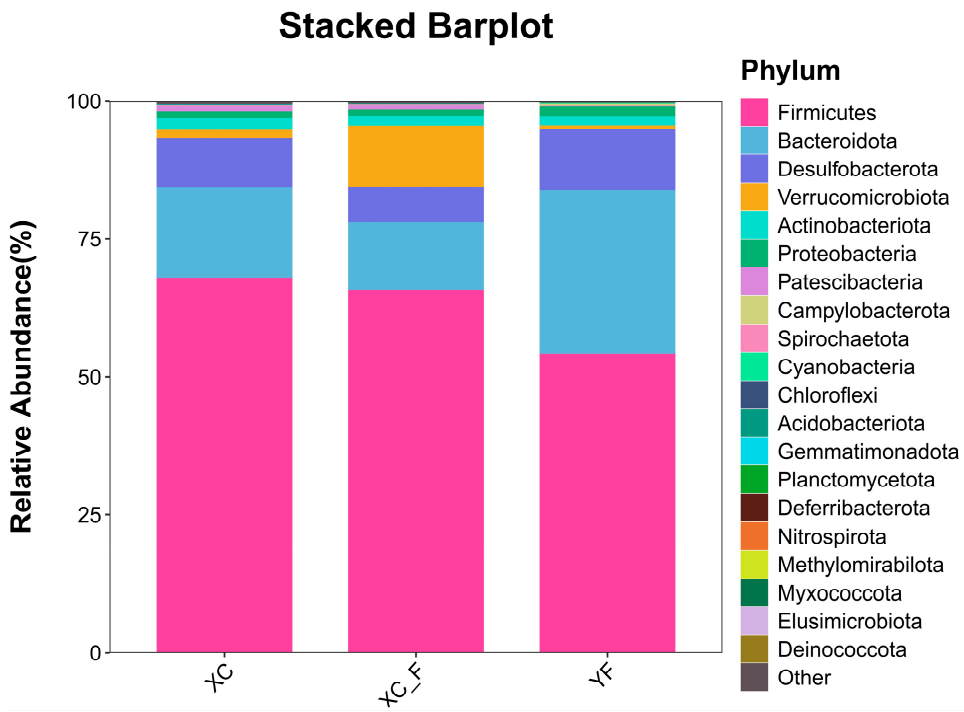


Figure 7. The species composition of intestinal microorganisms at the phylum level in different groups of Brandt's voles.

Based on the taxonomic annotation results of gut microbiota at the family level, the top 20 bacterial families ranked by relative abundance were selected to generate a z-score normalized relative abundance heatmap. As shown in Figure 8, the differential bacterial families across the XC, XC_F, and YF groups mainly belonged to the phyla Firmicutes, Bacteroidota, Desulfobacterota, and Verrucomicrobiota, and also covered taxa from Actinobacteriota, Patescibacteria, and Proteobacteria. The abundance profiles of bacterial families exhibited distinct clustering patterns and clear inter-group differentiation across treatments. Lachnospiraceae was the absolute dominant family in all three groups, belonging to the order Lachnospirales, class Clostridia, phylum Firmicutes. Its relative abundances were 26.26% in the XC group, 23.24% in the XC_F group, and 15.75% in the YF group, showing a stepwise decreasing trend. The heatmap showed a higher relative abundance of this family in XC than in YF. Muribaculaceae was the second most dominant family across groups, belonging to the order Bacteroidales, class Bacteroidia, phylum Bacteroidota. Its relative abundance rose sharply to 28.52% in the YF group, far higher than the levels in the XC group (15.05%) and the XC_F group (11.34%), presenting a pattern of specific enrichment in the YF group on the heatmap. Both Ruminococcaceae and Oscillospiraceae belong to the class Clostridia within the phylum Firmicutes, and maintained relatively high abundance in all three groups. Ruminococcaceae reached its highest relative abundance in the XC_F group at 12.47%, compared with 10.42% in the XC group and 10.61% in the YF group. The relative abundance of Oscillospiraceae followed a decreasing trend of XC group (9.22%) > XC_F group (8.51%) > YF group (6.70%). Desulfovibrionaceae, belonging to the order Desulfovibrionales, class Desulfovibrionia, phylum Desulfobacterota, had the highest relative abundance of 11.05% in the YF group, significantly higher than the levels in the XC group (9.16%) and the XC_F group (6.60%). The relative abundance of Akkermansiaceae (order Verrucomicrobiales, class Verrucomicrobiae, phylum Verrucomicrobiota) was 1.40% in XC, 11.06% in XC_F, and 0.63% in YF. Other low-abundance families with relative abundance below 2.0% also displayed distinct inter-group distribution patterns,

further verifying significant structural differentiation of gut microbiota among the three groups at the family level.

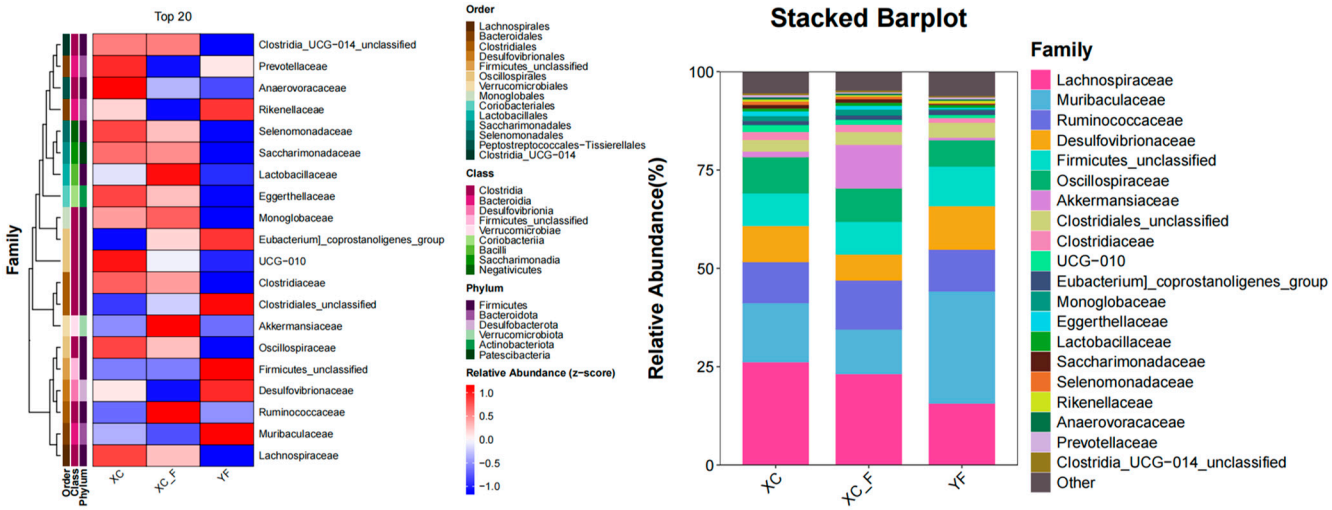


Figure 8. The species composition of intestinal microorganisms at the family level in different groups of Brandt's voles.

The stacked bar plot of species composition at the genus level (Figure 9) revealed distinct inter-group differentiation in gut microbiota community structure at the genus level among the three groups, and the relative abundance of dominant genera showed gradient changes corresponding to dietary treatments. Among all taxa, unclassified Muribaculaceae was the most abundant group across the three groups, with the highest relative abundance in the YF group, which was significantly higher than that in the XC and XC_F groups. The abundance of *Desulfovibrio* followed a decreasing trend of YF group > XC group > XC_F group, and was significantly enriched in the pure small-ruminant faeces feeding group. Lachnospiraceae_NK4A136_group was the second dominant genus, with its abundance maintained at relatively high levels in the XC and XC_F groups, but significantly decreased in the YF group. The relative abundance of *Ruminococcus* showed an increasing trend with the elevated proportion of small-ruminant faeces supplementation, reaching the highest level in the YF group. At day 21, the mean relative abundance of *Akkermansia* was 11.06% in the forage-plus-faeces group (XC_F) and 1.40% in the forage-only group (XC). The mean relative abundance in the faeces-only group (YF), sampled at its day-4 humane endpoint, was 0.63%. The Scheirer–Ray–Hare test detected an overall effect of dietary group ($H_{(2)}$ = 8.873, p = 0.01184). The main effect of sex ($H_{(1)}$ = 1.642, p = 0.20005) and the group-by-sex interaction ($H_{(2)}$ = 0.2423, p = 0.88590) were not statistically significant. With sexes pooled, the BH-adjusted p values were 0.0568 for XC versus XC_F, 0.318 for XC versus YF, and 0.0524 for XC_F versus YF (Figure 9). In the same comparison order, the adjusted p values were 0.800, 1.000, and 0.800 in females and 0.0536, 0.310, and 0.0536 in males. None of the pairwise comparisons met the 0.05 significance threshold.

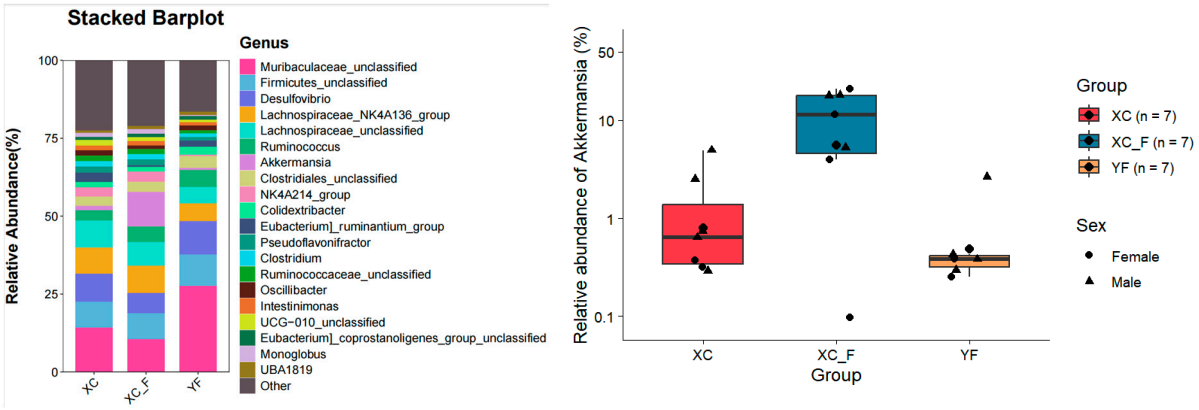


Figure 9. The species composition of intestinal microorganisms at the genus level in different groups of Brandt's voles. Note: The box plot shows the relative abundance of *Akkermansia* in the three dietary groups ($n = 7$ per group). Each point represents one vole, with circles denoting females and triangles denoting males. The vertical axis is logarithmic. The BH-adjusted p values from the pairwise Wilcoxon rank-sum tests were 0.0568 for XC versus XC_F, 0.318 for XC versus YF, and 0.0524 for XC_F versus YF. *Akkermansia* was detected in the sheep faeces profile (F1) at a relative abundance of 10.40%. The phylum-, family-, and genus-level profiles of F1 and the vole caecal samples are shown in Figure S2.

3.2.3. Analysis of Gut Microbiota Diversity Across Different Groups

One-way analysis of variance (ANOVA) showed that both the Chao1 index and Shannon index of gut microbiota in Brandt's voles exhibited highly significant inter-group differences among the three groups ($p < 0.001$). No significant difference was found in the Chao1 index between the XC group (1377.0) and the XC_F group (1390.7), and both were significantly higher than that of the YF group (835.0, both adjusted $p < 0.001$). The mean Shannon diversity values were 8.94 in XC, 8.44 in XC_F, and 7.70 in YF. Shannon diversity was significantly higher in XC and XC_F than in YF (adjusted $p < 0.001$ and adjusted $p = 0.023$, respectively), with no significant difference between XC and XC_F (adjusted $p = 0.151$). Chao1 richness and Shannon diversity were also analysed by ANCOVA with sex as a covariate. After adjustment for sex, the differences in α-diversity among the three groups remained highly statistically significant (Chao1: $F_{(2,17)} = 14.59$, $p < 0.001$; Shannon: $F_{(2,17)} = 12.90$, $p < 0.001$). Sex itself had no significant main effect on either α-diversity index ($p > 0.05$).

Permutational multivariate analysis of variance (PERMANOVA) based on Bray–Curtis distance was applied to evaluate differences in the overall gut microbiota community structure among the three groups. The overall PERMANOVA indicated significant differences among the three groups ($R^2 = 0.268$, $p = 0.001$). A permutational analysis of multivariate dispersions (PERMDISP) was further conducted to assess the homogeneity of multivariate dispersions among groups. The test revealed a highly significant difference in community dispersion across the three treatments ($F = 12.514$, $p < 0.001$). Post hoc Tukey HSD comparisons indicated no significant difference in within-group dispersion between the XC and XC_F groups (p_adj = 0.620), while the YF group exhibited significantly higher dispersion than both the XC group (p_adj = 0.004) and the XC_F group (p_adj < 0.001). YF was sampled at the day-4 humane endpoint, and XC and XC_F were sampled on day 21. Microbiota differences involving YF may reflect the combined effects of the faeces-only diet, earlier sampling, and physiological stress associated with low food intake and rapid body mass loss. Visualization via principal coordinates analysis (PCoA) revealed (Figure 10C) that the first principal coordinate (PCoA1) explained 21.7% of the microbiota variation. Samples from the pure small-ruminant faeces group (YF) were clearly separated from the other two groups along the PCoA1 axis. Samples from the two forage-based groups (XC and XC_F) partially

overlapped in the PCoA ordination (Figure 10C). Analysis of similarities (ANOSIM) further verified the significance of inter-group differences ($R = 0.6378$, $p = 0.001$), confirming that inter-group differences in community structure were significantly greater than intra-group individual differences. We also fitted a marginal PERMANOVA with dietary group and sex as predictors. After adjustment for sex, the explanatory power of dietary treatment on microbiota structure remained highly statistically significant ($R^2 = 0.266$, $p = 0.001$), while sex itself contributed minimally to microbiota variation with no statistical significance ($R^2 = 0.038$, $p = 0.518$).

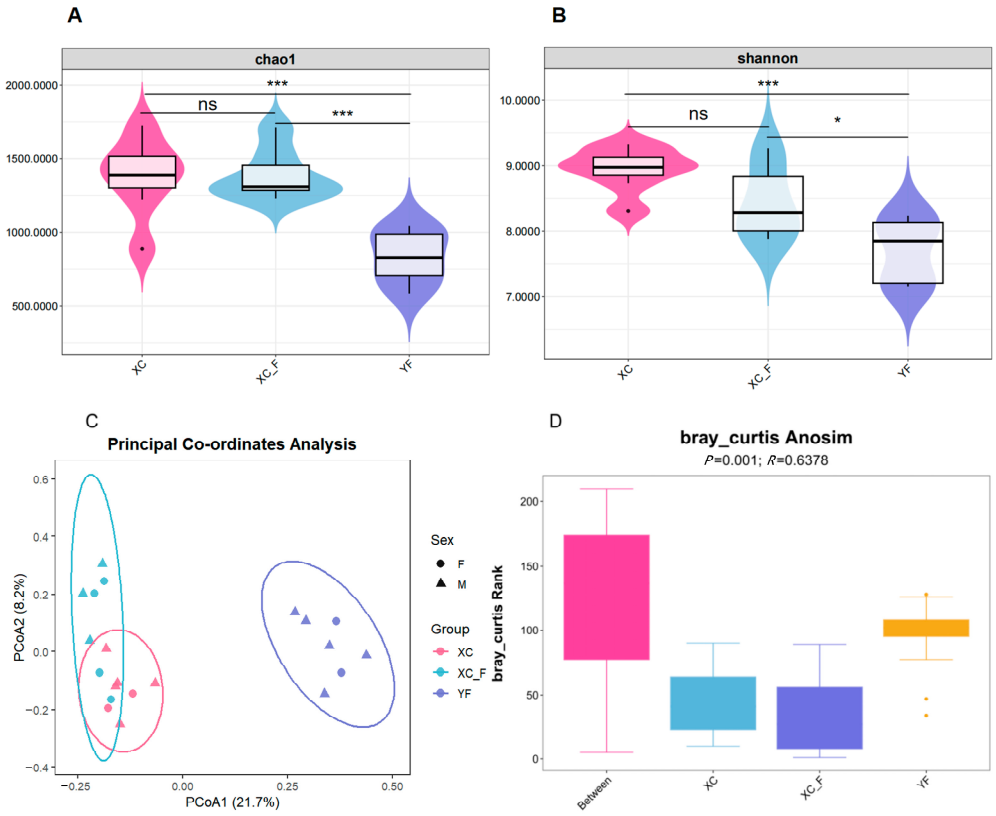


Figure 10. Analysis diagram of the species diversity of intestinal microorganisms in different groups. Note: Panels (**A**,**B**) show Chao1 richness and Shannon diversity, respectively. Brackets indicate pairwise comparisons from Tukey's HSD tests. ns indicates $p > 0.05$, * indicates $p < 0.05$, and *** indicates $p < 0.001$. Panels (**C**,**D**) show the beta-diversity analyses.

3.2.4. Functional Prediction and Differential Analysis of Gut Microbiota

Differences in the abundance of functional pathways among groups were tested using the Wilcoxon rank-sum test, with multiple comparisons corrected via the Benjamini–Hochberg (BH) method. Functional profile prediction was performed using PICRUSt2 based on 16S rRNA sequencing data. All results presented below are bioinformatic inferences, and actual metabolic activities require further experimental validation. The KEGG functional annotation results from PICRUSt2 showed that the core functional architectures of the three groups were highly similar. Among metabolic modules, carbohydrate metabolism and amino acid metabolism accounted for the highest proportions, while functions including membrane transport, translation, replication, and repair also maintained relatively high abundances (Figure 11). At the third-level pathway level, the top six pathways ranked by abundance were ABC transporters, ribosome, two-component system, purine metabolism, quorum sensing, and amino sugar and nucleotide sugar metabolism. The average relative abundances of ABC transporters were 4.13% in the XC group, 4.08% in the XC_F group,

and 3.51% in the YF group, with significantly higher levels in the XC and XC_F groups than in the YF group (adjusted $p < 0.05$). The average abundances of the two-component system in the three groups were 3.51%, 3.38%, and 3.28%, respectively, showing a decreasing trend of XC group > XC_F group > YF group, with statistically significant inter-group differences ($p < 0.05$). For quorum sensing, the average abundances in the three groups were 2.33%, 2.31%, and 2.12%, respectively, and the YF group was significantly lower than the other two groups ($p < 0.05$).

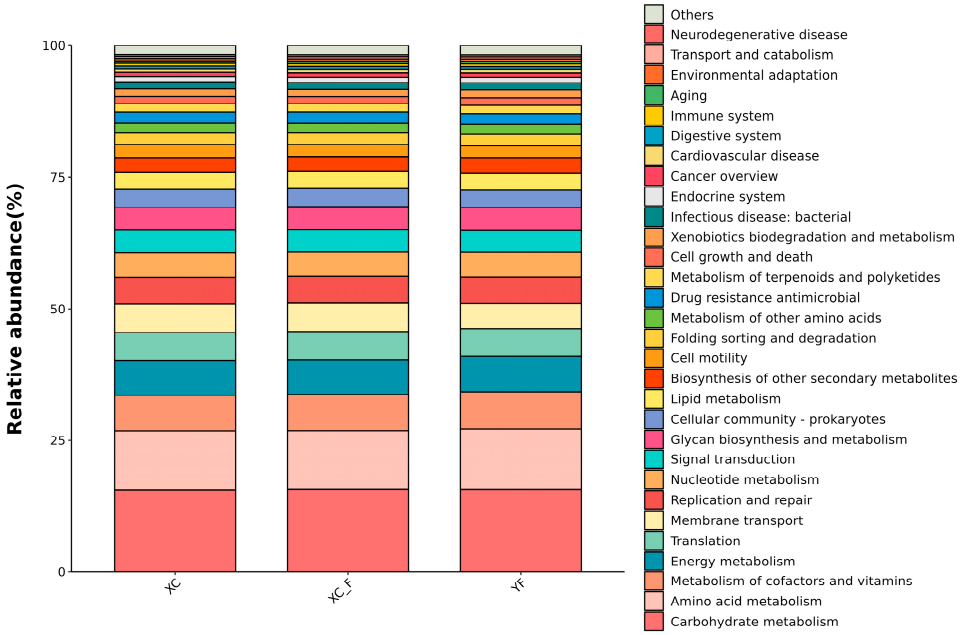


Figure 11. Relative abundance composition of KEGG functional categories in gut microbiota of different groups of Brandt's voles.

LEfSe analysis with the one-against-all multi-class comparison strategy identified group-associated differences in the PICRUSt2-predicted KEGG functional pathway profiles (Figure 12). The YF group was associated with basal energy metabolic pathways, including lipopolysaccharide biosynthesis, pyruvate metabolism, and the tricarboxylic acid cycle. The XC_F group was associated with carbohydrate transport and metabolism pathways, such as amino sugar and nucleotide sugar metabolism and the phosphotransferase system (PTS). The XC group was associated with pathways associated with substance transport and environmental response, represented by ABC transporters and the two-component system.

CAZy annotations of the PICRUSt2-predicted functional profiles covered six categories of carbohydrate-active enzymes and associated modules. Glycoside hydrolases (GH) accounted for the largest share in XC, XC_F, and YF (55.01%, 55.12%, and 56.72%, respectively), followed by glycosyltransferases (GT) (36.10%, 36.06%, and 35.21%, respectively). The remaining categories were carbohydrate-binding modules (CBM), carbohydrate esterases (CE), polysaccharide lyases (PL), and auxiliary activities (AA).

At the family level, Figure 13 shows 30 predicted CAZy families retained by one-against-all LEfSe at a nominal Kruskal–Wallis $p < 0.05$ and an LDA score > 2.0. Sixteen families were associated with XC, seven with XC_F, and seven with YF. The three highest LDA scores in XC were for GH13, CBM48, and GH38. The corresponding families were GT4, GH33, and CBM50 in XC_F and GH3, GT3, and GH31 in YF. Mean predicted relative abundances of GH13 in XC, XC_F, and YF were 13.40%, 13.21%, and 12.22%, respectively. The corresponding means for GH3 were 5.92%, 5.46%, and 6.93%.

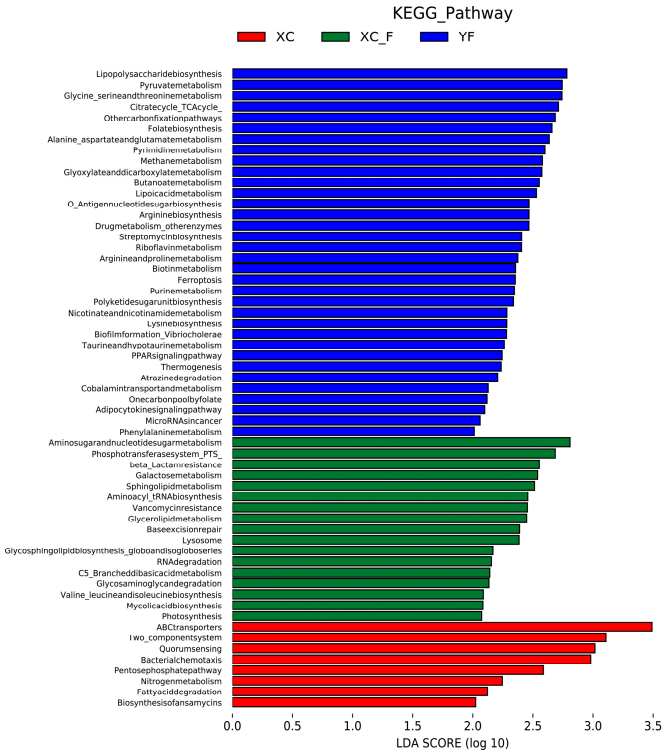


Figure 12. LEfSe analysis of differential KEGG metabolic pathways in gut microbiota of different groups of Brandt's voles.

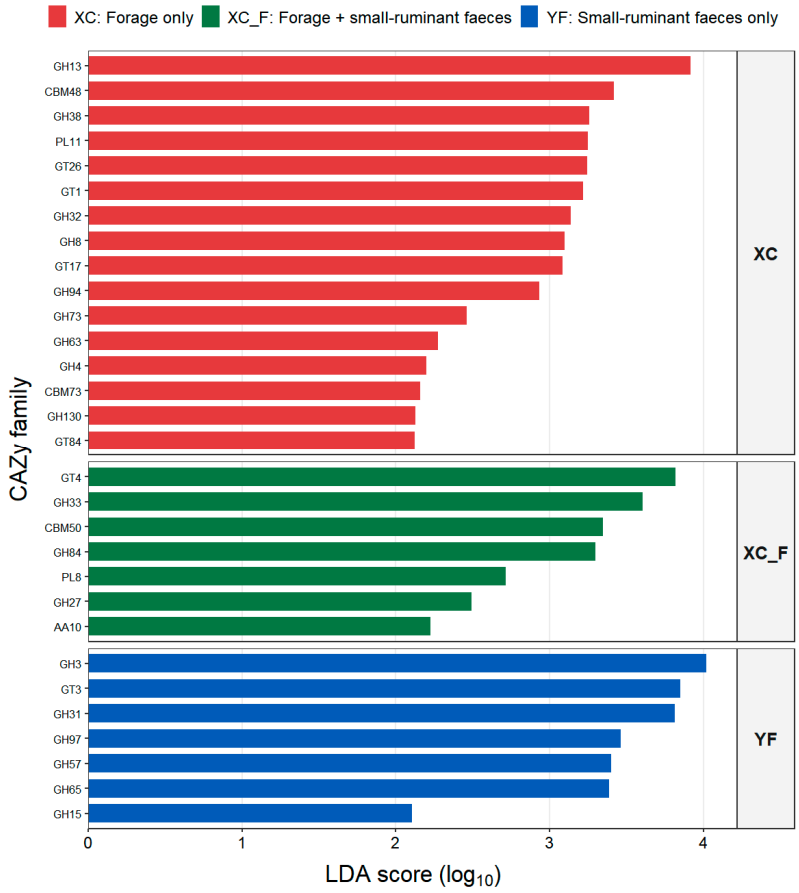


Figure 13. LEfSe analysis of predicted CAZy families in the caecal microbiota of Brandt's voles. The y-axis lists family identifiers from the Carbohydrate-Active enZymes (CAZy) database. GH, GT, CBM, PL, and AA denote glycoside hydrolases, glycosyltransferases, carbohydrate-binding modules,

polysaccharide lyases, and auxiliary activities, respectively. The number after each prefix identifies the family. Bar lengths represent logarithmic linear discriminant analysis (LDA) scores. The plotted families met the nominal Kruskal–Wallis threshold ($p < 0.05$) and the LDA score threshold (>2.0). XC (red) denotes forage only, XC_F (green) denotes forage plus small-ruminant faeces, and YF (blue) denotes small-ruminant faeces only.

MetaCyc annotation of the PICRUSt2-predicted functional profiles indicated a shared background of biosynthetic and energy-related pathways across the three vole groups. LEfSe analysis identified group-associated differences in the predicted pathway profiles. Among the 128 pathways reported in the differential-results table, 22 were associated with the XC group, 50 with the XC_F group, and 56 with the YF group under the criteria of an LDA score > 2 and a BH-adjusted q-value < 0.05. The five pathways with the highest LDA scores for each group are shown in Figure 14. In the XC group, the highest-ranking pathways were peptidoglycan maturation containing meso-diaminopimelate, the non-oxidative branch of the pentose phosphate pathway I, adenosine nucleotides degradation II, the superpathway of purine deoxyribonucleosides degradation, and the superpathway of N-acetylneuraminate degradation. Peptidoglycan maturation containing meso-diaminopimelate had the highest LDA score in this group (LDA = 2.796, $p = 0.001999$, $q = 0.009137$). The XC_F group was primarily associated with 4-amino-2-methyl-5-diphosphomethylpyrimidine biosynthesis II, the superpathway of sulfate assimilation and cysteine biosynthesis, thiamine diphosphate salvage IV, assimilatory sulfate reduction I, and anhydromuropeptides recycling II. The highest LDA score was observed for 4-amino-2-methyl-5-diphosphomethylpyrimidine biosynthesis II (LDA = 3.003, $p = 0.039924$, $q = 0.043103$). The YF group was characterized by group-associated pathways related to phosphatidylcholine acyl editing, the incomplete reductive TCA cycle, L-arginine biosynthesis III via N-acetyl-L-citrulline, the C4 photosynthetic carbon assimilation cycle (NAD-ME type), and ppGpp metabolism. Phosphatidylcholine acyl editing showed the highest LDA score among the YF-associated pathways (LDA = 3.018, $p = 0.000402$, $q = 0.005914$).

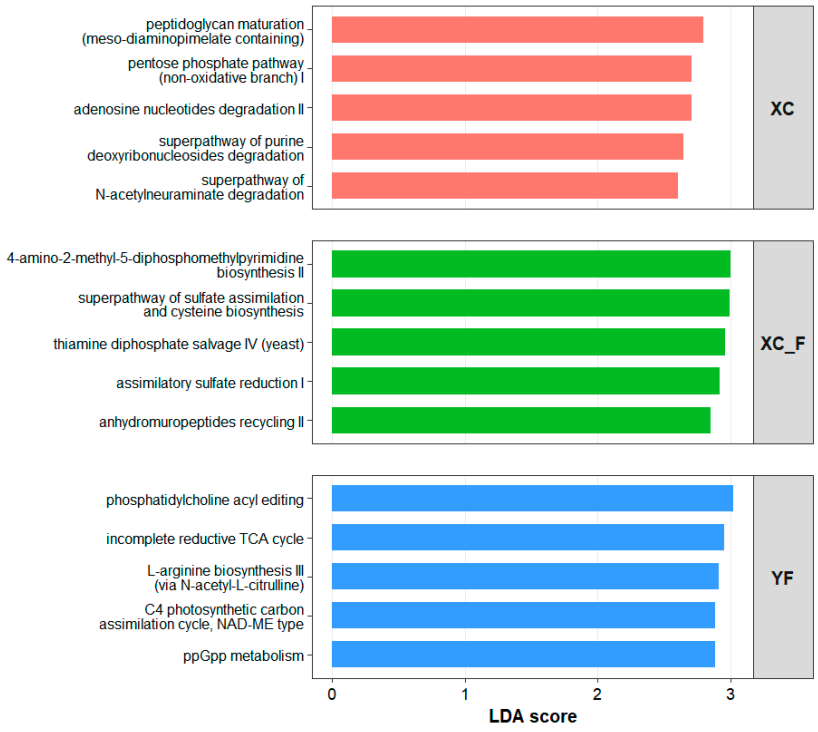


Figure 14. Top five group-associated PICRUSt2-predicted MetaCyc pathways identified by LEfSe analysis. Note: Bars represent LDA scores. Pathways with LDA scores > 2 and BH-adjusted q-values < 0.05

were retained. XC denotes the forage-only group, XC_F denotes the forage plus field-collected small-ruminant-faeces group, and YF denotes the faeces-only group. The 128 screened MetaCyc pathway results are provided in Table S1.

4. Discussion

Small-ruminant faeces were found in 29 of 34 Brandt's vole burrow systems surveyed over six years. We found no statistically detectable association between the stored masses of plant food and small-ruminant faeces in the model accounting for survey year. The sensitivity analyses gave the same qualitative result. The surveys document the presence of faeces in food stores, whereas their subsequent consumption and the circumstances of their transport in the field remain unknown. Incidental transport with plant material, non-food use, and variation in local forage or faecal availability are plausible explanations. The feeding trial documents intake when faeces were offered alongside forage under laboratory conditions.

Direct observations and the detection of yak DNA in stomach contents supported yak faeces consumption by plateau pikas [8]. A comparative review documents a range of contexts in which vertebrates consume faeces [22]. For Brandt's voles, establishing field consumption of stored faeces would require direct observations or dietary evidence. Selective digesta retention [6] and direct observations of caecotrophy [23] document different aspects of faecal recycling in captive Brandt's voles. Experimental prevention of autocoprophagy also altered their gut microbiota [11]. Enclosure experiments linked sheep grazing to changes in vole diets and gut bacterial composition [9]. A separate feeding experiment linked variation in forage species richness and composition to differences in the gut microbiota of postweaning Brandt's voles [20]. Together, these studies provide a context for examining faeces recovered from burrow storage chambers.

When forage and faeces were offered separately, voles in the XC_F group consumed an average of 0.362 g of faeces per day, approximately 3.3% of their total intake by mass. Total daily food intake was lower in XC_F than in XC. Body mass increased over the 21-day trial in both groups, and final body mass did not differ significantly between them after adjustment for sex ($p = 0.065$). Faeces thus accounted for a small proportion of voluntary intake, and the trial provided no evidence of improved growth. The diets were offered to subadult voles at 20 ± 1 °C under a 14 h light and 10 h dark photoperiod. The trial did not measure dietary nutrient or energy content, apparent digestibility, feed conversion, or overwinter survival. A lamb trial on dried white mulberry pomace illustrates how intake, growth and feed conversion can be assessed together [24]. Assessing these endpoints in voles would help determine the nutritional consequences of ingesting small-ruminant faeces. On day 21, mean *Akkermansia* relative abundance was 11.06% in XC_F and 1.40% in XC. The pairwise comparison did not reach statistical significance after BH adjustment (adjusted $p = 0.0568$). This was a genus-level result from 16S rRNA amplicon sequencing. *Akkermansia muciniphila*, a characterised species within the genus, can use mucin as a substrate [25]. Experimental fasting increased *A. muciniphila* in Syrian hamsters [26]. Differences in food intake and substrate availability are possible explanations for the observed difference in group means and warrant further investigation. Relative abundance can also increase when other taxa decline, so absolute *Akkermansia* abundance cannot be inferred from these data [27]. *Akkermansia* was also detected in the profile of the sheep faeces used in the feeding trial (F1, three subsamples from one batch, Supplementary Figure S2). Its detection in both sample types is compatible with exposure to faecal microorganisms. The genus-level profiles cannot distinguish strain transfer or persistence from a response of resident vole microbiota. A comparison of feed and host samples at strain resolution, including host sampling before and after exposure, would help distinguish these possibilities [28]. The predicted KEGG profile associated XC_F with the phosphotransferase system and amino sugar and nucleotide sugar metabolism. Among the higher-ranking XC_F-associated MetaCyc predictions were path-

ways related to sulfate assimilation and thiamine metabolism. PICRUSt2 infers microbial functional potential from marker-gene profiles and reference genomes [29]. Furthermore, the mean relative abundances of Lachnospiraceae and Muribaculaceae were lower in XC_F than in XC. The taxonomic and predicted functional profiles therefore provide no direct evidence of greater short-chain fatty acid (SCFA) production or improved nutrient utilisation. Previous experiments in Brandt's voles have investigated microbiota-associated responses to cold, huddling and postnatal thermoregulation [5,12,30]. Our feeding trial did not include a cold exposure or measure caecal SCFAs, pH, ammonia, apparent digestibility or host energy expenditure. Future work could pair apparent digestibility with direct metabolite measurements, as illustrated by the use of a digestibility marker together with faecal pH, ammonia and SCFA measurements in a canine feeding study [31].

The overall Bray–Curtis analysis detected differences among the three groups. Dispersion also differed, with greater within-group dispersion in YF than in the two forage-based groups. We therefore interpret the overall PERMANOVA and ANOSIM results alongside the dispersion analysis, particularly for comparisons involving YF [32]. XC and XC_F were sampled on day 21 and partially overlapped in the ordination. In YF, caecal samples were collected on day 4 at early termination, after low intake and rapid weight loss. Studies in vertebrates show that fasting-related changes in gut microbiota can vary by host and intestinal compartment [33]. In this trial, diet, sampling day, and the physiological state at sampling were inseparable for YF. Its lower alpha diversity and higher relative abundance of Bacteroidota and Muribaculaceae describe the early endpoint under these combined conditions. The same-day XC and XC_F contrast provides the basis for discussing supplementation-associated differences.

Each treatment included seven voles, and microbiota profiling was limited to a single caecal endpoint per animal. The laboratory conditions also differed from winter conditions in the field. Direct observations in burrows or dietary evidence from wild voles would help establish whether stored faeces are consumed. For microbiota comparisons in future work, a common sampling schedule and matched intake controls would help distinguish responses to diet composition from those associated with lower intake or physiological stress.

5. Conclusions

Small-ruminant faeces were frequently detected in Brandt's vole food stores. In the laboratory, voles were offered forage, and faeces were consumed in small amounts. On day 21, the mean *Akkermansia* relative abundance was 11.06% in XC_F and 1.40% in XC (BH-adjusted $p = 0.0568$). Final body mass did not differ significantly between the groups. The faeces-only group reached a humane endpoint on day 4, limiting its microbiota comparison with the other treatments. The findings document faeces consumption under laboratory conditions and supplementation-associated microbiota differences. Their relevance to nutrient utilisation and winter survival remains to be determined.

Supplementary Materials: The following supporting information can be downloaded at: https://www.mdpi.com/article/10.3390/microorganisms14122769/s1. Figure S1. Model diagnostics for the field analysis of faecal storage mass. Figure S2. Taxonomic composition of the small-ruminant faecal samples and vole caecal microbiota. Table S1. Screened MetaCyc pathway results for the three feeding groups.

Author Contributions: Investigation, J.F., S.S., Q.W., Q.B., X.K., H.S., Z.C. and Q.L.; Conceptualization, J.F.; methodology, J.F.; writing—original draft preparation, J.F.; writing—review and editing, G.Y., S.Y. and H.F.; Funding acquisition, H.F. All authors have read and agreed to the published version of the manuscript.

Funding: This research was funded by the National Key Research and Development Program of China (2024YFD1400500); the Science and Technology Basic Resources Investigation Program of the Ministry of Science and Technology of China (2023FY100305); the Key Research and Development Project of Inner Mongolia Autonomous Region Science and Technology Plan (2025YFHH0177); and the Key Program of the Natural Science Foundation of Inner Mongolia Autonomous Region (2025ZD033).

Institutional Review Board Statement: The animal experimental protocol of this study was reviewed and approved by the Laboratory Animal Ethics Committee of Inner Mongolia Agricultural University (Approval No. NND2023081, approval date 6 March 2023). All experimental procedures were conducted in strict compliance with the 3Rs principles (Replacement, Reduction and Refinement) and conformed to the ARRIVE 2.0 guidelines. Field animal capture and burrow system surveys were carried out with permission from the local forestry and grassland administrative authority. A body weight loss exceeding 20% of the baseline body weight was predefined as the humane endpoint criterion. Animals were euthanized via cervical dislocation to minimize animal distress to the greatest extent possible.

Informed Consent Statement: Not applicable.

Data Availability Statement: The raw 16S rRNA gene amplicon sequencing reads from the 21 caecal content samples of Brandt's voles (*Lasiopodomys brandtii*) have been deposited in the NCBI Sequence Read Archive (SRA) under BioProject accession PRJNA1565328 and SRA Study accession SRP758050. The BioSample accessions are SAMN65454779–SAMN65454799, and the SRA Run accessions are SRR41885943–SRR41885963. The dataset is scheduled for public release six months after submission to NCBI.

Conflicts of Interest: The authors declare no conflicts of interest.

References

1. Shi, D.Z.; Hai, S.Z.; Jin, X.M.; Liu, X.L. Study on the Behavior Forage and Selection for Storage of Forage Plants of Brandt's Vole (*Microtus brandti*) Before Overwintering. *Acta Agrestia Sin.* **1997**, *5*, 20–26. [CrossRef]
2. Zhang, Z.; Bu, F.; Sun, S.; Ming, M.; Liu, T.; Li, Y.; Wu, X.; Zhang, X.; Yuan, S.; Fu, H. The Individual Division of Food Hoarding in Autumn Brandt's Voles (*Lasiopodomys brandtii*). *Animals* **2024**, *14*, 2719. [CrossRef] [PubMed]
3. Song, Y.; Li, G.; Zhang, Z. The Cooperative Food Hoarding Behaviors of Brandt's Voles and Their Influencing Factors. *Acta Theriol. Sin.* **2021**, *41*, 658–666. [CrossRef]
4. Zhang, X.Y.; Wang, D.H. Thermogenesis, Food Intake and Serum Leptin in Cold-Exposed Lactating Brandt's Voles *Lasiopodomys brandtii*. *J. Exp. Biol.* **2007**, *210*, 512–521. [CrossRef] [PubMed]
5. Zhang, X.Y.; Sukhchuluun, G.; Bo, T.B.; Chi, Q.S.; Yang, J.J.; Chen, B.; Zhang, L.; Wang, D.H. Huddling Remodels Gut Microbiota to Reduce Energy Requirements in a Small Mammal Species during Cold Exposure. *Microbiome* **2018**, *6*, 103. Erratum in *Microbiome* **2018**, *6*, 126. https://doi.org/10.1186/s40168-018-0509-1. [CrossRef] [PubMed]
6. Pei, Y.X.; Wang, D.H.; Hume, I.D. Selective Digesta Retention and Coprophagy in Brandt's Vole (*Microtus brandti*). *J. Comp. Physiol. B* **2001**, *171*, 457–464. [CrossRef] [PubMed]
7. Fish, K.D.; Sauther, M.L.; Loudon, J.E.; Cuozzo, F.P. Coprophagy by Wild Ring-Tailed Lemurs (*Lemur catta*) in Human-Disturbed Locations Adjacent to the Beza Mahafaly Special Reserve, Madagascar. *Am. J. Primatol.* **2007**, *69*, 713–718. [CrossRef] [PubMed]
8. Speakman, J.R.; Chi, Q.; Ołdakowski, Ł.; Fu, H.; Fletcher, Q.E.; Hambly, C.; Togo, J.; Liu, X.; Piertney, S.B.; Wang, X.; et al. Surviving Winter on the Qinghai-Tibetan Plateau: Pikas Suppress Energy Demands and Exploit Yak Feces to Survive Winter. *Proc. Natl. Acad. Sci. USA* **2021**, *118*, e2100707118. [CrossRef] [PubMed]
9. Li, G.; Li, J.; Kohl, K.D.; Yin, B.; Wei, W.; Wan, X.; Zhu, B.; Zhang, Z. Dietary Shifts Influenced by Livestock Grazing Shape the Gut Microbiota Composition and Co-occurrence Networks in a Local Rodent Species. *J. Anim. Ecol.* **2019**, *88*, 302–314. [CrossRef] [PubMed]
10. Li, G.; Yin, B.; Li, J.; Wang, J.; Wei, W.; Bolnick, D.I.; Wan, X.; Zhu, B.; Zhang, Z. Host-Microbiota Interaction Helps to Explain the Bottom-Up Effects of Climate Change on a Small Rodent Species. *ISME J.* **2020**, *14*, 1795–1808. [CrossRef] [PubMed]
11. Bo, T.B.; Zhang, X.Y.; Kohl, K.D.; Wen, J.; Tian, S.J.; Wang, D.H. Coprophagy Prevention Alters Microbiome, Metabolism, Neurochemistry, and Cognitive Behavior in a Small Mammal. *ISME J.* **2020**, *14*, 2625–2645. [CrossRef] [PubMed]
12. Bo, T.B.; Zhang, X.Y.; Wen, J.; Deng, K.; Qin, X.W.; Wang, D.H. The Microbiota–Gut–Brain Interaction in Regulating Host Metabolic Adaptation to Cold in Male Brandt's Voles (*Lasiopodomys brandtii*). *ISME J.* **2019**, *13*, 3037–3053. [CrossRef] [PubMed]
13. Shabana, I.I.; Albakri, N.N.; Bouqellah, N.A. Metagenomic Investigation of Faecal Microbiota in Sheep and Goats of the Same Ages. *J. Taibah Univ. Sci.* **2021**, *15*, 1–9. [CrossRef]

14. Emu, Q.; Guan, H.; Zhu, J.; Zhang, L.; Fan, J.; Ji, Y.; Lin, Y.; Li, C.; Dan, X.; Aguo, Y.; et al. Grazing and Supplementation of Dietary Yeast Probiotics Shape the Gut Microbiota and Improve the Immunity of Black Fattening Goats (*Capra hircus*). *Front. Microbiol.* **2021**, *12*, 666837. [CrossRef] [PubMed]
15. Cheong, S.; Aguirre-Siliezar, K.; Williams, S.R.; Gaudin, A.C.M.; Pagliari, P.; Jay-Russell, M.T.; Busch, R.; Maga, E.A.; Pires, A.F.A. Exploring the Impact of Grazing on Fecal and Soil Microbiome Dynamics in Small Ruminants in Organic Crop-Livestock Integration Systems. *PLoS ONE* **2025**, *20*, e0316616. [CrossRef] [PubMed]
16. Ming, M.; Yuan, S.; Fu, H.; Li, X.; Zhang, H.; Liu, T.; Bu, F.; Wu, X. Influence of biotic and abiotic factors on flea species population dynamics on *Lasiopodomys brandtii*. *Int. J. Parasitol. Parasites Wildl.* **2023**, *21*, 185–191. [CrossRef] [PubMed]
17. Wang, J.; Wang, S.-S.; Qiao, X.-G.; Li, A.; Xue, J.-G.; Hasi, M.; Zhang, X.-Y.; Huang, J.-H. Influence of nitrogen addition on the primary production in Nei Mongol degraded grassland. *Chin. J. Plant Ecol.* **2016**, *40*, 980–990. [CrossRef]
18. Dong, L.; Li, G.C.; Wang, B.; Lu, L.; Zhao, N.; Wan, X.R.; Liu, W.; Hu, B.; Xing, A.; Li, Q.D.; et al. An investigation of chigger mites on rodents in the grasslands of eastern Inner Mongolia Autonomous Region, China. *Chin. J. Vector Biol. Control* **2022**, *33*, 873–878. [CrossRef]
19. Zhu, H.; Li, G.; Liu, J.; Xu, X.; Zhang, Z. Gut microbiota is associated with the effect of photoperiod on seasonal breeding in male Brandt's voles (*Lasiopodomys brandtii*). *Microbiome* **2022**, *10*, 194. [CrossRef] [PubMed]
20. Li, G.; Shi, C.; Song, Y.; Chu, H.; Zhang, Z. The Role Transition of Dietary Species Richness in Modulating the Gut Microbial Assembly and Postweaning Performance of a Generalist Herbivore. *mSystems* **2021**, *6*, e00979-21. [CrossRef] [PubMed]
21. Percie du Sert, N.; Hurst, V.; Ahluwalia, A.; Alam, S.; Avey, M.T.; Baker, M.; Browne, W.J.; Clark, A.; Cuthill, I.C.; Dirnagl, U.; et al. The ARRIVE Guidelines 2.0: Updated Guidelines for Reporting Animal Research. *PLoS Biol.* **2020**, *18*, e3000410. [CrossRef] [PubMed]
22. Power, E.J.; Bornbusch, S.L.; Kendrick, E.L. Faeces as food: A framework for adaptive nutritional coprophagy in vertebrates. *Anim. Behav.* **2024**, *218*, 75–86. [CrossRef]
23. Liu, Q.-S.; Li, J.-Y.; Wang, D.-H. Ultradian rhythms and the nutritional importance of caecotrophy in captive Brandt's voles (*Lasiopodomys brandtii*). *J. Comp. Physiol. B* **2007**, *177*, 423–432. [CrossRef] [PubMed]
24. Inanc, Z.S.; Arik, H.D. Effects of dried white mulberry pomace on fattening performance and metabolic profile parameters in lambs. *Eurasian J. Vet. Sci.* **2025**, *41*, e0464. [CrossRef]
25. Derrien, M.; Vaughan, E.E.; Plugge, C.M.; de Vos, W.M. *Akkermansia muciniphila* gen. nov., sp. nov., a human intestinal mucin-degrading bacterium. *Int. J. Syst. Evol. Microbiol.* **2004**, *54*, 1469–1476. [CrossRef] [PubMed]
26. Sonoyama, K.; Fujiwara, R.; Takemura, N.; Ogasawara, T.; Watanabe, J.; Ito, H.; Morita, T. Response of gut microbiota to fasting and hibernation in Syrian hamsters. *Appl. Environ. Microbiol.* **2009**, *75*, 6451–6456. [CrossRef] [PubMed]
27. Vandeputte, D.; Kathagen, G.; D'hoe, K.; Vieira-Silva, S.; Valles-Colomer, M.; Sabino, J.; Wang, J.; Tito, R.Y.; De Commer, L.; Darzi, Y.; et al. Quantitative microbiome profiling links gut community variation to microbial load. *Nature* **2017**, *551*, 507–511. [CrossRef] [PubMed]
28. Smillie, C.S.; Sauk, J.; Gevers, D.; Friedman, J.; Sung, J.; Youngster, I.; Hohmann, E.L.; Staley, C.; Khoruts, A.; Sadowsky, M.J.; et al. Strain tracking reveals the determinants of bacterial engraftment in the human gut following fecal microbiota transplantation. *Cell Host Microbe* **2018**, *23*, 229–240.e5. [CrossRef] [PubMed]
29. Douglas, G.M.; Maffei, V.J.; Zaneveld, J.R.; Yurgel, S.N.; Brown, J.R.; Taylor, C.M.; Huttenhower, C.; Langille, M.G.I. PICRUSt2 for prediction of metagenome functions. *Nat. Biotechnol.* **2020**, *38*, 685–688. [CrossRef] [PubMed]
30. Bo, T.; Tang, L.; Xu, X.; Liu, M.; Wen, J.; Lv, J.; Wang, D. Role of gut microbiota in the postnatal thermoregulation of Brandt's voles. *Cell Rep.* **2023**, *42*, 113021. [CrossRef] [PubMed]
31. Kahraman, O.; İnal, F.; Alataş, M.S.; İnanç, Z.S.; Damar, S.; Ahmed, I.; Uludağ, M.; Çalıkoğlu, T. Substitution of poultry fat with black soldier fly (*Hermetia illucens*) larvae fat in dog diets: Effects on digestibility, palatability, peroxidation of dry food, immunity, blood biochemistry, and faecal characteristics of adult dogs. *Vet. Sci.* **2025**, *12*, 311. [CrossRef] [PubMed]
32. Anderson, M.J.; Walsh, D.C.I. PERMANOVA, ANOSIM, and the Mantel test in the face of heterogeneous dispersions: What null hypothesis are you testing? *Ecol. Monogr.* **2013**, *83*, 557–574. [CrossRef]
33. Kohl, K.D.; Amaya, J.; Passement, C.A.; Dearing, M.D.; McCue, M.D. Unique and shared responses of the gut microbiota to prolonged fasting: A comparative study across five classes of vertebrate hosts. *FEMS Microbiol. Ecol.* **2014**, *90*, 883–894. [CrossRef] [PubMed]

Disclaimer/Publisher's Note: The statements, opinions and data contained in all publications are solely those of the individual author(s) and contributor(s) and not of MDPI and/or the editor(s). MDPI and/or the editor(s) disclaim responsibility for any injury to people or property resulting from any ideas, methods, instructions or products referred to in the content.